sustainability

MDPI

Article

Synergistic Integration of EVs and Renewable DGs in Distribution Micro-Grids

Mahmoud Ghofrani

Division of Engineering and Mathematics, School of STEM, University of Washington, Bothell, WA 98011, USA; mrani@uw.edu; Tel.: +1-425-352-3224

Abstract: This paper proposes a multi-objective optimization framework for safe, reliable, and economic integration of electric vehicles (EVs) and renewable distributed generators (DGs) in distribution micro-grids. EV and DG coordination optimization with the use of vehicle-to-grid (V2G) technology along with system reconfiguration optimization is developed to provide collective revenues and address integrational complications that may occur by additional system loading due to EV charging and EV-DG energy exchanges. A Genetic Algorithm (GA) optimizes the EV charging/discharging in synergies with renewable DGs to maximize benefits that can be captured by their collaborative participation in electricity market and through renewable energy arbitrage. The developed EV charging/discharging optimization is implemented in a real 134-bus distribution network and is evaluated for its potential operational implications, namely, increased system losses. A system reconfiguration is then proposed to reduce the system losses by optimizing the flow of power through switching on/off the connections within the micro-grid and/or with other distribution systems. Simulation results demonstrate the efficiency of the proposed method in not only providing collective revenues, but also in enhancing the system operation by reducing the losses of the distribution grid. The collective benefits proposed by the developed optimization and validated by the simulation results facilitate transitioning to clean and eco-friendly sources of energy for generation and transportation, which in turn leads to more sustainable development of societies and communities.

Keywords: distribution network; electric vehicles; GA optimization; operation; planning; reconfiguration; renewable distributed generators

Citation: Ghofrani, M. Synergistic Integration of EVs and Renewable DGs in Distribution Micro-Grids. *Sustainability* **2024**, *16*, 3939. https://doi.org/10.3390/su16103939

Academic Editors: Marcelo Gustavo Molina and Maximiliano Martinez

Received: 30 March 2024
Revised: 21 April 2024
Accepted: 7 May 2024
Published: 8 May 2024

1. Introduction

The widespread integration of renewable energy sources (RESs) and electric vehicles (EVs) into exiting distribution grids offers potential economic, environmental, and societal benefits for energy entities. The economic benefits are provided through participating in electricity markets where EVs can purchase renewable generation more than the scheduled generation for charging during off-peak periods and sell the stored energy at a higher price during peak periods or when the renewable generation falls behind the schedule. This market participation benefits RESs by reducing penalties associated with renewable over- and under-production. The increased utilization of renewable provides an additional revenue stream for RESs in the form of production tax credits and reduces green-house gas emissions. Nevertheless, technical issues of EV and RES integration have been detrimental in capturing these benefits. Variability of RESs, such as wind and solar, is one of the technical challenges that make it difficult to balance fluctuations in energy production with consumer demand. The challenge is exacerbated by existing EV charging practices that are mainly unidirectional from the grid to the EV. Unlike bi-directional charging, which enables energy exchange between EVs and RESs to offset their fluctuations, unidirectional charging has limits in responding flexibly and efficiently to such fluctuations. Even with the bidirectional charging, the interaction between EVs and renewable energy needs to recognize their synergies with other energy entities to maximize the benefits offered by such

interaction. Furthermore, strains that EVs charging/discharging place on the grid and its operation need to be addressed. Together, the combination of the technical difficulties and intricacy of the problem given the high number of involved entities and their individual needs has made it challenging to efficiently integrate RESs and EVs and optimize their operations to maximize the collective benefits for all participants while minimizing adverse impacts of their integration.

Integration of renewable distributed generators (DGs) and EVs in distribution systems has been extensively studied in the literature. Numerous methods were developed to address key integration challenges, including voltage deviations, excessive loading, increased losses, power quality issues, renewable generation, and EV driving volatilities, etc. These methods can be classified into three major categories, namely: coordination, capacitor optimization, and system reconfiguration.

The coordination method refers to optimal charging/discharging of EVs in recognition of renewable fluctuations to alleviate uncertainties of EV driving patterns and renewable generation. The coordination can be based on market objective [1–4] or to address operational issues [5–7]. The market objective is to take advantage of renewable arbitrage and provide revenues for renewable DGs and EVs. The operational challenges stem from an improper integration of EVs and DGs into distribution grids, which result in augmented power losses and voltage deviations, among other issues.

The capacitor optimization method is to optimally size and place capacitors across the distribution networks to address voltage-related issues such as voltage deviations, stability, over- and under-voltages, etc. [8–10]. This method has proven effective in improving the voltage profile of the grid. However, the capacitor investment cost and possible transient instability of the system due to capacitor operation degrade the potential benefits that can be captured by this method.

The system reconfiguration adjusts the physical layout of the distribution network by closing and/or opening the normally open tie and/or normally close sectionalizing switches, respectively, as well as reconfiguring paths to optimize the flow of power. The objective is to enhance the system operation by reducing system losses, improving voltage/frequency profile, etc. Distribution network reconfiguration in the presence of EVs and RESs has been investigated in several studies [11–14]. The existing reconfiguration methods are mainly applicable to stand-alone micro-grids and internal interactions only. This neglects the connections among different distribution systems and the fact that coordinating EVs and RESs within one system could affect the operation of other connected systems.

Despite the large body of literature for the individual categories, the combination of these methods for optimizing EV and renewable DG integration has not been adequately investigated. This is mainly due to the high number of energy entities within the distribution network that makes it difficult to efficiently capture their synergies and to provide collective benefits for all participants rather than benefiting individual entities.

This paper proposes an optimization framework that combines the coordination and system reconfiguration methods for EV and renewable DG integration. Even though there are several existing tools for individual integration of EVs and renewable DGs, there are a lack of tools for their combined and synergistic integration [15,16]. The proposed optimization addresses the pressing needs of the energy industry for an EV and RES integration tool with the capability to:

- Capture synergies among all energy entities and participants.
- Recognize the interconnection of distribution micro-grids to provide a global optimization for the interconnected grids rather than a local optimum for a single micro-grid.
- Integrate technical, economic, and market objectives into system operation for EV charging/discharging to provide collective benefits and incentives for all participants rather than individual benefits for the system operator or utility company only.
- Employ for real-time or low-time demanding applications such as power flow analysis.

The developed tool can be used by several different players, including planners, distribution operators, utilities, independent system operators (ISOs), policymakers, etc., to quantify and evaluate the effects of EVs and RES integration, and to address the negative impacts accordingly. This facilitates the transition to more sustainable and environmentally friendly energy generation and transportation.

The paper is organized as follows. Section 2 presents the methods. Section 3 provides the case studies and simulation results. Conclusions are given in Section 4.

2. Methods

This project proposes to develop a hierarchical optimization framework for coordinating EVs charging/discharging with the operation of micro-grid energy entities. The proposed hierarchy decomposes the complex optimization with multiple objectives and a high number of participants and decision variables into different layers of optimization with decoupled economic and operation objectives. The economic objective is to maximize the benefits that micro-grid energy entities can capture by their collaborative participation in the electricity market and through energy arbitrage. To this end, an autoregressive-moving-average (ARMA) model is proposed to characterize random uncertainties of renewable generation and EV driving patterns. The Monte Carlo simulation (MCS) simulates system states based on the developed ARMA models. A Genetic Algorithm (GA) then optimizes the EV charging/discharging in coordination with other energy entities. The combination of ARMA model, MCS, and GA provides a stochastic optimization to satisfy the proposed economic objective.

The operation objective is to minimize technical complications such as increased system losses that a distribution micro-grid may incur due to additional loading and energy exchanges caused by EV charging/discharging. To this end, a binary optimization is proposed to reconfigure the distribution micro-grid and its interconnection with other distribution systems by optimally switching on/off the connections within the micro-grid and/or with other distribution systems.

The following flowchart demonstrates the proposed hierarchical optimization (Figure 1).

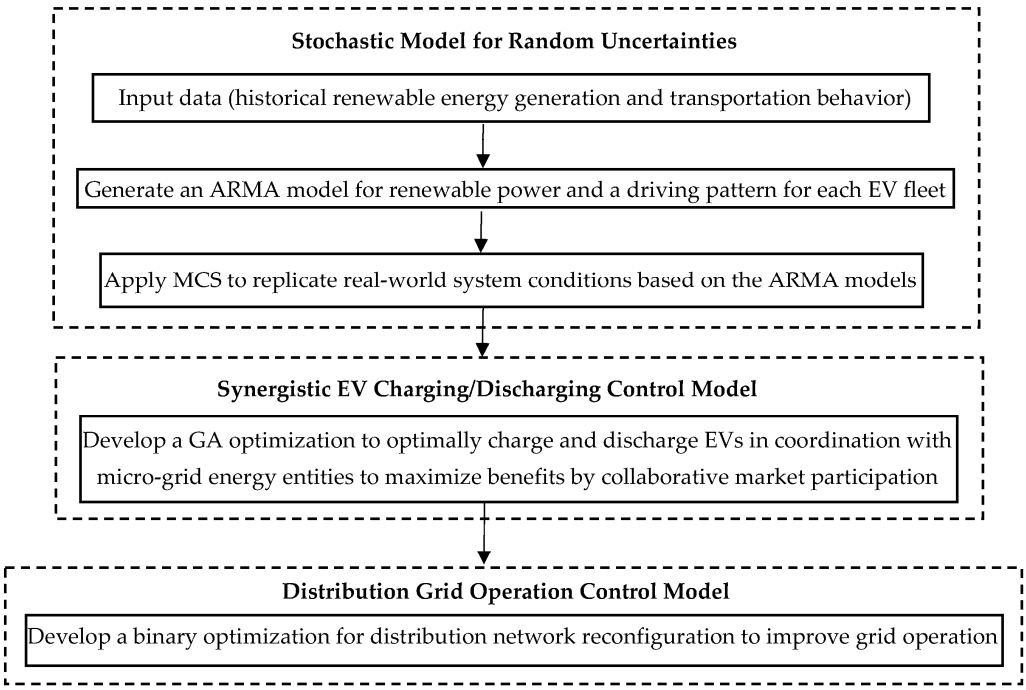

Figure 1. Schematic diagram of the optimized integration method for EVs and renewable DGs.

The following sections present the methods employed for developing the proposed optimization framework.

2.1. Stochastic Variables

Stochastic variables are random quantities that introduce uncertainty in their frequency of changes. The wind and solar power generation and EV driving patterns are the stochastic variables in this study. Despite forecasting advancements, inherent uncertainty and forecast errors persist, leading to potential instances of inadequate and excessive renewable generation. Such inaccuracies can translate into costly under- and over-production penalties for renewable DGs, which ultimately degrade their economic benefits. Therefore, accurate modelling of the stochastic variables is essential to identify their uncertainties and reduce the operation cost of the system. The models used in this study for renewable DGs and EVs are as follows.

2.1.1. ARMA Model for Renewable DGs

Wind speed and solar radiation are known for their unpredictable fluctuations over time. To mimic these stochastic variations, an ARMA model is used in this paper due to its high accuracy, ease of implementation, and parameter selection [17]. The ARMA model relies on historical hourly wind speed and clearness index data. These data are used to calculate the autoregressive (AR) and moving average (MA) coefficients [18].

$$x_t = \sum_{n=1}^{N} \varnothing_n x_{t-n} + \sum_{m=1}^{M} \theta_m \alpha_{t-m} \tag{1}$$

Equations (2) and (3) are then used to alter the wind speed and clearness index time series to the mean (μ_t) and standard deviation (σ_t) of the recorded hourly data to generate an authentic representation of the wind speed and clearness index numerically.

$$W_t = \mu_{W_t} + x_{W_t}.\sigma_{W_t} \tag{2}$$

$$K_t = \mu_{K_t} + x_{K_t}.\sigma_{K_t} \tag{3}$$

The wind and solar DG power outputs are calculated using the following Equations: [19].

$$P_{W-DG} = \begin{cases} 0 & v \le v_{cut-in}, v \ge v_{cut-out} \\ \frac{v - v_{cut-in}}{v_{rated} - v_{cut-in}} P_{W-DG_{rated}} & v_{cut-in} \le v \le v_{rated} \\ P_{W-DG_{rated}} & v_{rated} \le v \le v_{cut-out} \end{cases} \tag{4}$$

$$P_{PV-DG} = A_{PV} \times \eta_{PV} \times \left(T \times K_t - T' \times K_t^2 \right) \tag{5}$$

The proposed modelling of wind and solar DG effectively captures the inherent randomness of these variables, making the system analysis and optimization more accurate.

2.1.2. Driving Model for EV

To effectively model the effect of EV loads on distribution systems, driving and charging patterns must be taken into consideration. Historical data about driving patterns is used to model the charging/discharging power of the EV battery which is subject to the following inequality constraints [19]:

$$|P_c(t_c)| \le P_c^{max} \quad \forall c \in L \tag{6a}$$

$$|P_d(t_d)| \le P_d^{max} \quad \forall d \in L \tag{6b}$$

This paper utilizes Fuzzy C-Means (FCM) clustering to group EVs into separate fleets, highlighting significant similarities in driving behaviors [19]. FCM does not use

mathematical distribution to characterize data; rather, it is a technique used for data pattern recognition and similarities.

2.2. Monte Carlo Simulation

MCS is used in this paper to replicate the real-world scenarios by generating samples of wind and solar generation and EV driving/charging patterns. These samples are generated based on the stochastic models developed in Section 2.1. The samples are then utilized as the inputs into the objective function (f) to calculate the outputs (Y) of MCS, i.e., simulated states. The relation between the inputs and outputs of MCS is as follows:

$$Y = f(P_{W-DG}, P_{PV-DG}, P_c, P_d) \tag{7}$$

The simulation is repeated, and the average values of the simulated states are calculated at the end of each scenario. This process halts upon achieving convergence, at which point the average values do not further change by repeating the simulation for an additional scenario.

2.3. Synergistic EV Charging/Discharging Control Model

A coordination method is developed in this section to optimize the EV charging/ discharging in collaboration with renewable DGs. The proposed coordination maximizes the synergies between EVs and renewable DGs to provide collective benefits for the involved energy entities. The benefits are captured by EVs' and DGs' participation in a bilateral contract and through renewable arbitrage. The participation involves EVs to use the renewable power more than the scheduled generation for charging. The excess energy can be purchased at low market prices, as it would otherwise result in over-production penalties for renewable DGs. While not in use, the EVs can discharge the stored energy through V2G to compensate for renewable shortages when DGs generate less than what they are scheduled for. The discharged energy can be sold at higher market clearing prices, as the power shortage usually occurs during peak load events. The proposed participation not only benefits EVs through renewable arbitrage but provides revenues for renewable DGs. The DG revenues are two fold: a reduction in penalties for renewable over- and under-production, and incentives in the form of production tax credits (PTC) due to increased utilization of renewable generation. The collective benefits are given by the following Equations:

$$R_{EV} = P_d(t_d) \times \Delta t_d \times MCP(t_d) - P_c(t_c) \times \Delta t_c \times MCP(t_c) \;\; \forall c, d \in L \tag{8}$$

$$R_{DG} = PTC_{DG} - PEN_{DG} \tag{9}$$

$$PEN_{DG}(t_k) = \begin{cases} (P_{Sch.-DG}(t_k) - P_{Act.-DG}(t_k)) \times (1.1 \cdot MCP(t_k)) & for\ DG\ under-production \\ (P_{Act.-DG}(t_k) - P_{Sch.-DG}(t_k)) \times (0.1 \cdot MCP(t_k)) & for\ DG\ over-production \end{cases} \tag{10}$$

The 1.1 and 0.1 coefficients in Equation (10) are associated with the Federal Energy Regulatory Commission (FERC), and its mandate to settle the intermittent resources' imbalances at 90% and 110% of decremental and incremental costs, respectively [20,21].

A GA optimization is used to maximize the collective revenues by the market participants, as follows:

$$Obj.Function = Max\{R_{EV} + R_{DG}\} \tag{11}$$

2.4. Distribution Grid Operation Control Model

The efficient and reliable planning and operation of distribution grids in the presence of EVs and DGs require a control model that addresses the increased feeder loading and the consequent increased losses due to the EV charging. The developed synergistic EV charging/discharging control model and the subsequent continuous exchange of energy between EVs and DGs can result in even more significant losses in distribution grids. To evaluate the operational implications of the EV charging/discharging control model

and quantify the distribution grid losses, a load flow analysis is used in this paper. A distribution system reconfiguration optimization is then proposed to adjust connections within the distribution network using two types of switches: tie, and sectionalizing. Tie switches are typically open and are used to provide connections among different feeders if needed. Sectionalizers are normally closed switches that will open to avoid creation of any loops and maintain the radial structure of the distribution grid after the tie switches close to serve a feeder from other feeder(s). The objective of the operation control model is to minimize the distribution system losses by optimally closing and opening the tie and sectionalizing switches, respectively.

$$Obj.Function = Min(P_{Loss}) = Min\left(\sum_{l=1}^{(N_{br}+N_{ts})} x_l I_l^2 R_l\right) \quad (12)$$

The objective function is subject to the following equality and inequality constraints.

2.4.1. Node Voltage Constraints

The operating voltage at each bus (i) of the distribution network must adhere to the standard limits, as follows:

$$v_i^{min} \leq v_i \leq v_i^{max} \quad (13)$$

This paper assumes the 0.95–1.05 standard range for the bus voltages [22].

2.4.2. Feeder Capacity Constraints

The power flowing through each branch of the network must not exceed the branch's current capacity.

$$I_l \leq I_l^{max} \qquad l\varepsilon\{1, 2, 3, \ldots, \ldots, N_{br} + N_{ts}\} \quad (14)$$

2.4.3. Bus Isolation Constraints

All network buses must be served upon reconfiguration. Therefore, none of the buses can undergo isolation without being supplied by a feeder. This requires only one switch to open in a loop.

2.4.4. Network Configuration Constraints

The reconfigured distribution network must maintain a radial configuration. To this end, the reconfiguration must prohibit the creation of any loops in the network. The following equality constraint ensures that the system is radially operated upon reconfiguration [23].

$$\sum_1^{(N_{br}+N_{ts})} x_l = N_b - 1 \quad (15)$$

2.4.5. Power Balance Constraints

The active and reactive power must be balanced in the reconfigured network. This requires adequate generation of active/reactive power to supply the active/reactive load and compensate for the active/reactive losses of the reconfigured network. These constraints are satisfied by the following power balance Equations.

$$\sum P_i^{Gen} = P_{Loss} + \sum P_i^{Load} \quad (16a)$$

$$\sum Q_i^{Gen} = Q_{Loss} + \sum Q_i^{Load} \quad (16b)$$

GA is used in this section to optimize the system configuration and minimize the losses of the reconfigured network.

3. Case Studies and Simulation Results

3.1. Test System

A 13.8 kV, 134-bus real distribution network is used to evaluate the performance of the proposed hierarchical optimization. The single-line diagram of the network is

shown in Figure 2 [24]. The network includes five feeders with normally open tie switches between buses 38–46, 63–76, 78–89, and 90–119. The impedance matrices of different conductor/tower types and Thevenin equivalent of the external network are as follows:

$$Z_{\text{equivalent}} = \begin{bmatrix} 0.2900 + i \cdot 1.9200 & 0.1960 + i \cdot 0.5300 & 0.1960 + i \cdot 0.5300 \\ 0.1960 + i \cdot 0.5300 & 0.2900 + i \cdot 1.9200 & 0.1960 + i \cdot 0.5300 \\ 0.1960 + i \cdot 0.5300 & 0.1960 + i \cdot 0.5300 & 0.2900 + i \cdot 1.9200 \end{bmatrix} \Omega$$

$$Z_{\#4/0}\ (\text{in blue}) = \begin{bmatrix} 0.4272 + i \cdot 0.9609 & 0.0600 + i \cdot 0.4780 & 0.0600 + i \cdot 0.4500 \\ 0.0600 + i \cdot 0.4780 & 0.4272 + i \cdot 0.9609 & 0.0600 + i \cdot 0.5360 \\ 0.0600 + i \cdot 0.4500 & 0.0600 + i \cdot 0.5360 & 0.4272 + i \cdot 0.9609 \end{bmatrix} \Omega/\text{km}$$

$$Z_{\#1/0}\ (\text{in green}) = \begin{bmatrix} 0.7567 + i \cdot 1.0067 & 0.0600 + i \cdot 0.4780 & 0.0600 + i \cdot 0.4500 \\ 0.0600 + i \cdot 0.4780 & 0.7567 + i \cdot 1.0067 & 0.0600 + i \cdot 0.5360 \\ 0.0600 + i \cdot 0.4500 & 0.0600 + i \cdot 0.5360 & 0.7567 + i \cdot 1.0067 \end{bmatrix} \Omega/\text{km}$$

$$Z_{\#4}\ (\text{in black}) = \begin{bmatrix} 1.6440 + i \cdot 1.0060 & 0.0600 + i \cdot 0.4780 & 0.0600 + i \cdot 0.4500 \\ 0.0600 + i \cdot 0.4780 & 1.6440 + i \cdot 1.0060 & 0.0600 + i \cdot 0.5360 \\ 0.0600 + i \cdot 0.4500 & 0.0600 + i \cdot 0.5360 & 1.6440 + i \cdot 1.0060 \end{bmatrix} \Omega/\text{km}$$

$$Z_{\#2}\ (\text{in red}) = \begin{bmatrix} 1.0840 + i \cdot 0.9980 & 0.0600 + i \cdot 0.4780 & 0.0600 + i \cdot 0.4500 \\ 0.0600 + i \cdot 0.4780 & 1.0840 + i \cdot 0.9980 & 0.0600 + i \cdot 0.5360 \\ 0.0600 + i \cdot 0.4500 & 0.0600 + i \cdot 0.5360 & 1.0840 + i \cdot 0.9980 \end{bmatrix} \Omega/\text{km}$$

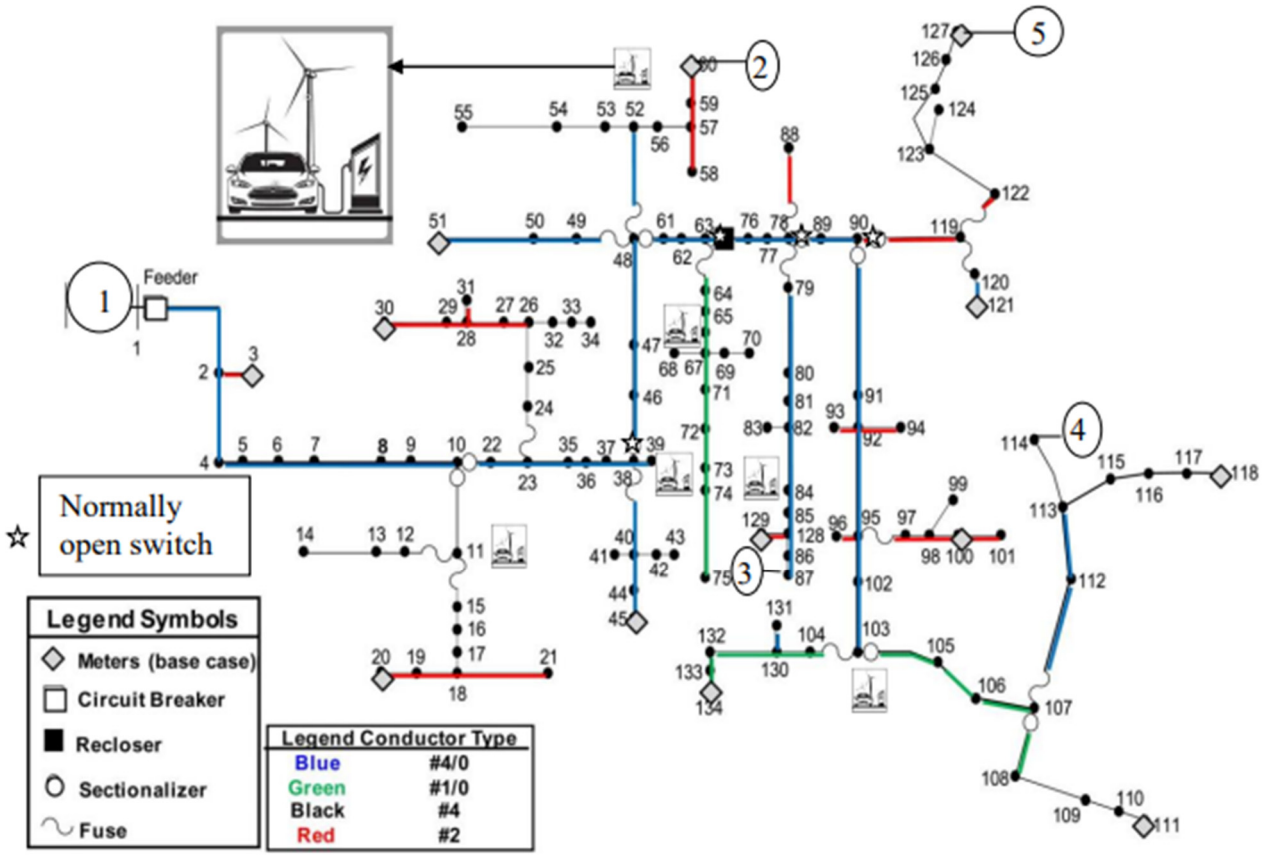

Figure 2. Single-line diagram of the test network.

Table 1 provides the lines and load data for the 134-bus distribution network, where k and m represent the initial and final bus of each branch.

Table 1. Lines and load data for the 134-bus distribution test system.

k	*m*	Dist. (m)	S_{load} (kVA)	*k*	*m*	Dist. (m)	S_{load} (kVA)
1	2	900	0	67	69	20	7
2	3	50	45	69	70	20	112.5
2	4	100	0	67	71	50	75
4	5	40	75	71	72	40	8.5
5	6	200	75	72	73	40	1.9
6	7	200	112.5	73	74	20	112.5
7	8	200	75	74	75	110	112.5
8	9	10	75	63	76	20	112.5
9	10	50	0	76	77	30	5.9
10	11	100	0	77	78	50	0
11	12	60	8.6	78	79	70	75
12	13	30	75	79	80	70	112.5
13	14	1 60	75	80	81	30	112.5
11	15	30	112.5	81	82	30	0
15	16	10	45	82	83	50	75
16	17	20	112.5	82	84	50	75
17	18	40	0	84	85	30	112.5
18	19	40	75	85	128	20	0
19	20	50	112.5	128	86	30	15.5
18	21	150	112.5	86	87	20	75
10	22	30	112.5	78	88	130	75
22	23	70	0	78	89	50	75
23	24	50	3	89	90	50	0
24	25	20	45	90	91	180	45
25	26	30	0	91	92	20	0
26	27	60	112.5	92	93	30	112.5
27	28	40	0	92	94	70	23.5
28	29	20	75	92	95	100	0
29	30	120	112.5	95	96	40	75
28	31	20	112.5	95	97	50	6
26	32	20	112.5	97	98	60	0
32	33	5	112.5	98	99	110	23.5
33	34	25	112.5	98	100	40	75
23	35	10	0	00	101	110	112.5
35	36	70	12.4	95	102	60	112.5
36	37	10	112.5	102	103	40	0
37	38	10	0	103	104	30	75
38	39	70	3	103	105	150	75
38	40	100	0	105	106	210	108.5
40	41	60	75	106	107	30	0
40	42	50	75	107	108	100	0
42	43	10	75	108	109	100	108.5
40	44	30	112.5	109	110	30	112.5
44	45	40	45	110	I11	20	112.5
38	46	60		107	112	170	75
46	47	20	112.5	112	113	110	0
47	48	120	0	113	114	110	0
48	49	50	112.5	113	115	200	30
49	50	20	75	115	116	200	30
50	51	170	112.5	116	117	200	30
48	52	100	0	117	118	200	30
52	53	60	1.2	90	119	110	0

Table 1. *Cont.*

k	*m*	Dist. (m)	S_{load} (kVA)	*k*	*m*	Dist. (m)	S_{load} (kVA)
53	54	30	112.5	119	120	70	0
54	55	130	75	120	121	70	30
52	56	20	75	119	122	70	55
56	57	80	0	122	123	130	0
57	58	50	10	123	124	20	15.5
57	59	60	112.5	123	125	20	15.5
59	60	20	3.8	125	126	40	45
48	61	40	3	126	127	40	112.5
61	62	10	5.5	128	129	60	45
62	63	50	0	104	130	70	0
63	64	30	75	130	131	20	112.5
64	65	20	75	130	132	100	0
65	66	30	3.5	132	133	40	112.5
66	67	20	0	133	134	40	112.5
67	68	30	112.5				

3.2. Synergistic EV Charging/Discharging

In total, 10 MW renewable generation capacity is installed on six buses within the test distribution network. Three wind power units with 0.85 power factor are installed at buses 67, 84, and 103, and three solar PV units with 0.95 power factor are installed at buses 11, 39, and 52. The 10 MW capacity is evenly distributed among the wind power and solar PV units. The MCS is used to generate 1000 scenarios whose average determine the renewable DG generation for a 24 h simulation period. In total, 484 EVs are grouped into six fleets of similar driving patterns and distributed within the test network. EV charging stations are co-located with the renewable DGs to facilitate the EV-DG coordination. The EVs are equipped with V2G capabilities, enabling them to function as loads or generators, depending on charging or discharging status. GA is utilized to optimally charge and discharge EVs in coordination with DGs to maximize their collective revenues. An hourly interval set is used for the simulation to make it consistent with the energy cost time resolution that is usually provided and applied in the energy industry. This assumption enables the calculations of economic revenues that EVs and renewable DGs capture by their participation in the energy arbitrage market. Figure 3 provides the EV charging/discharging optimization results for the simulation period. Status of charges (SOCs) are calculated for each EV fleet for 1000 MCS scenarios and are averaged to calculate the hourly power. The SOCs of the consecutive hours are then subtracted to determine the charging/discharging power for the EV fleets. Positive values indicate EV charging from the grid to EVs, while negative values signify EV discharging into the grid. Some values are very close to zero, correlating to a negligible power exchange and minimal power flow. The EV used in this study has a battery with a power rating of 6 kW. The average power varies for different fleets based on the number of EVs within each fleet determined by the FCM clustering, and their optimal charging/discharging power determined by the synergistic EV charging/discharging control model.

Figure 4 shows the hourly energy cost that is used to calculate the collective revenues from EVs and renewable DGs. Table 2 provides the revenues that are captured by the developed synergistic EV charging/discharging control model. The simulation results in this Table demonstrate the potential for substantial financial gains as incentives for EVs and renewable DGs to participate in the energy arbitrage market. However, the additional loading of the system due to EV charging and recurring flow of power between EVs and DGs can potentially increase the system losses. The issue can be addressed by optimizing the distribution grid operation to mitigate the losses. To this end, the control model developed in Sections 2–4 will be used to structurally reconfigure the 134-bus network.

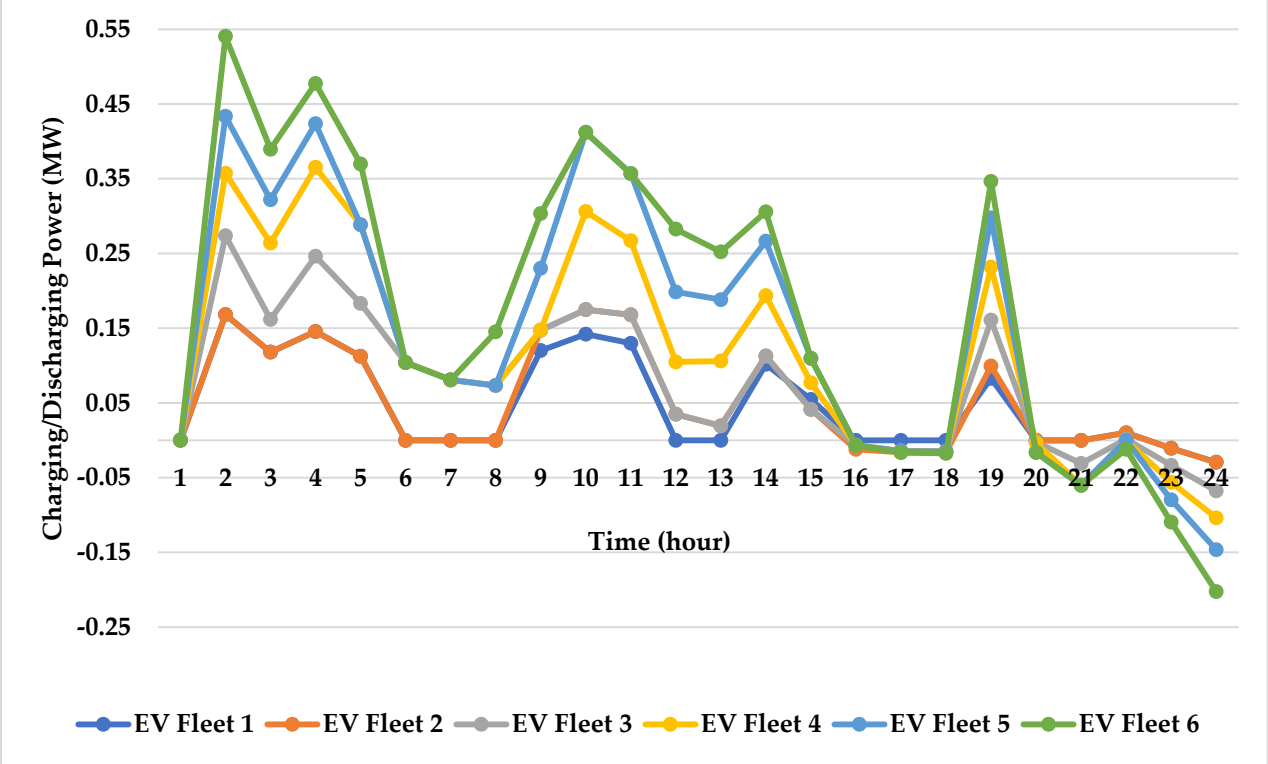

Figure 3. Optimal charging/discharging of the EV fleets for the 24-h simulation period.

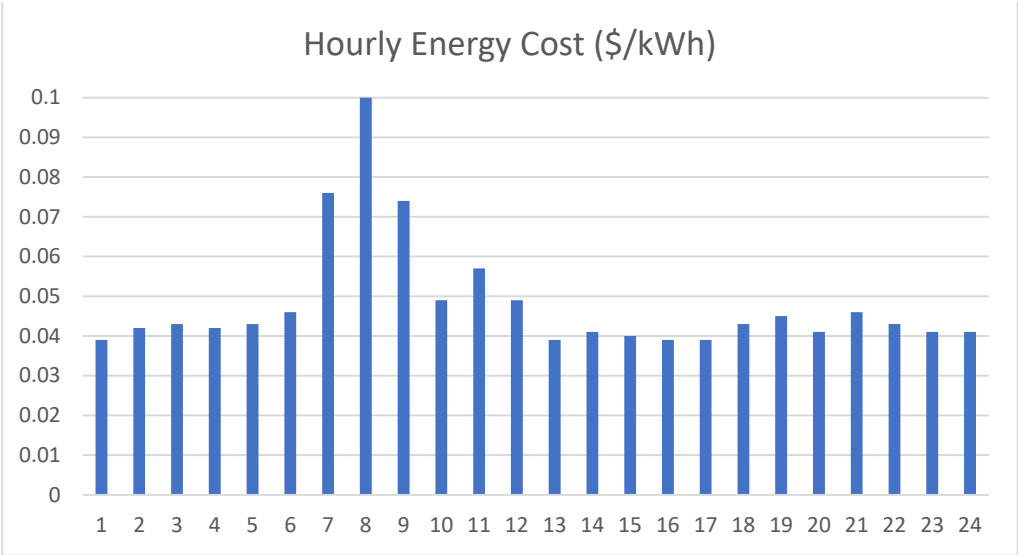

Figure 4. Energy cost for the 24 h simulation period.

Table 2. Collective revenues of EVs and renewable DGs for the 24 h simulation period.

EV Fleet & Renewable DG @ Bus#	11	39	52	67	84	103
(R_{EV} + R_{DG})($)	202	99	204	197	167	173

3.3. Distribution Grid Operation

Five feeders are included in the 134-bus distribution network to represent the connections with neighboring distribution systems and to reflect the interconnected nature of energy systems. Two types of switches are modeled in the distribution network: tie switches, and sectionalizing switches. The tie switches are the four switches between buses

38–46, 63–76, 78–89, and 90–119 of the 134-distribution network which are normally open. Unlike the tie switches, the sectionalizing switches are normally closed. Interconnecting the distribution networks by closing any combination of the tie switches is accompanied by opening a combination of sectionalizing switches to ensure that the radial structure of the reconfigured network is upheld without creating any loops.

The proposed distribution grid operation control model is used to determine the optimal combinations of tie and sectionalizing switches that need to be closed and opened, respectively, to minimize the system losses. Due to heterogeneity of overhead lines and unbalanced loads of the system, an unbalanced three-phase power flow analysis is performed for the original 134-bus network and the reconfigured system to calculate their power losses. These calculations quantify the loss reduction that is achieved by the proposed reconfiguration optimization. Table 3 provides the optimization results for hourly switching actions over the 24 h simulation period. The bus numbers between which the switches are located along with the associated line number are indicated in the Table. The results demonstrate that the proposed optimization not only includes the existing switches, but also places new sectionalizing switches between buses 62–63, 89–90, 95–102, and 102–103, and optimizes their actions. This results in the most efficient operation of the system by reducing the system losses to its minimum. The total number of switches that are proposed to operate for loss reduction is 11. Comparing the switching actions for consecutive hours display the proposed operation of the system. For example, the normally open switch between buses 90 and 119 (located on line 121) is proposed to close at hour 1. Then, it needs to open at hour 2 and remain open for hour 3. The proposed switching action for hour 4 is closing. The switch must stay close for hours 5 and 6, followed by an opening switching action at hour 7. An idle operation is proposed for hours 8 through 15, i.e., the switch remains open for these hours. The next switching action is to close the switch at hour 16 which is kept closed for the next 4 h. The switch is proposed to open at hour 21 without any further actions for the remainder of the simulation period.

Table 3. Distribution network reconfiguration optimization for the 24 h simulation period.

Hr	Switch 10–22 Line 23	Switch 38–46 Line 47	Switch 61–48 Line 62	Switch 62–63 Line 64	Switch 63–76 Line 77	Switch 78–89 Line 91	Switch 89–90 Line 92	Switch 95–102 Line 104	Switch 102–103 Line 105	Switch 105–106 Line 108	Switch 90–119 Line 121
1	OPEN	CLOSE		OPEN	CLOSE	CLOSE	OPEN	OPEN			CLOSE
2			OPEN	CLOSE			CLOSE	CLOSE	OPEN		OPEN
3											
4							OPEN	OPEN	CLOSE		CLOSE
5											
6											
7							CLOSE	CLOSE	OPEN		OPEN
8											
9											
10											
11											
12								CLOSE	OPEN		
13											
14											
15								OPEN	CLOSE		
16							OPEN				CLOSE
17								CLOSE	OPEN		
18											
19											
20								OPEN	CLOSE		
21							CLOSE				OPEN
22											
23											
24								CLOSE		OPEN	

Table 4 provides an analysis of the system losses before reconfiguration and after the switching actions. The difference between the losses before and after the optimization is calculated and provided in terms of MW and percentage loss reduction. Shaded regions in these tables are idle operations for the switches, i.e., no switching actions. There is no loss reduction for the hours with idle switching operation, as the system configuration and the consequent system losses do not change. The simulation results for loss reductions support the proposed system reconfiguration method for addressing the minimization of losses upon executing the synergistic EV charging/discharging method.

Table 4. Pre- and post-optimization losses.

Hr	Loss-Original Network (MW)	Loss-Reconfigured Network (MW)	Loss Reduction (MW)	Loss Reduction (%)
1	0.108167	0.057842	−0.050325	−46.525060
2	0.056311	0.055286	−0.001026	−1.821358
3				
4	0.077036	0.076748	−0.000288	−0.374996
5				
6				
7	0.057888	0.057099	−0.000789	−1.362655
8				
9				
10				
11				
12	0.056467	0.056285	−0.000181	−0.321111
13				
14				
15	0.049949	0.049886	−0.000063	−0.125808
16	0.065659	0.065922	0.000263	0.401094
17	0.082846	0.082818	−0.000027	−0.032776
18				
19				
20	0.076921	0.076774	−0.000147	−0.191446
21	0.053192	0.052306	−0.000886	−1.665252
22				
23				
24	0.030322	0.030253	−0.000069	−0.227400

Based on the simulation results, the reconfiguration optimization can be classified into the following categories.

3.3.1. Planning Optimization

The switching actions for hour 1 provide the most drastic results with 46.52% reduction in losses upon system reconfiguration. This is mainly due to the proposed eight switching actions and the consequent significant changes in system configuration. As such, the placement of the new sectionalizing switches and the actions associated with this hour can be considered as a planning strategy.

3.3.2. Real-time Operation Optimization

The loss reductions for hours 2–24 are insignificant, as they pertain to real-time EVs and renewable DGs output changes in a one-hour timeframe. Therefore, the switching actions for hours 2–24 can be used for real-time operation optimization. This real-time operation demonstrates a reduction in the total number of switching occurrences where system optimization is still achieved but at a lower percentage.

The collective revenue results of Table 2, along with the loss reduction results of Table 4, prove the accuracy of the proposed method as an economical- and technical-oriented approach to facilitate the integration of clean and zero-emission energy resources

including renewable DGs and EVs. This, in combination with the potential environmental and societal benefits, offers an integrated approach for clean and sustainable development in energy and transportation sectors as the two main contributing sectors to GHG emissions.

4. Conclusions

A multi-objective hierarchical optimization is developed in this paper to integrate and operate renewable DGs and EVs in distribution grids efficiently and reliably. The developed method simulates real-world system states by stochastically modeling uncertainties such as renewable generation and EV driving patterns. An EV charging/discharging control model is proposed to optimize synergies between EVs and DGs and maximize their collaborative revenues. A distribution network reconfiguration optimization is then developed to address technical challenges associated with the implementation of the proposed EV charging/discharging control along with the operation of EVs and DGs. The developed hierarchical optimization is tested on a real 134-bus distribution system, and its performance is assessed by comparing the pre- and post-optimization results. Simulation results demonstrate economic revenues by synergistic EV charging/discharging optimization, as well as loss reduction by optimal system reconfiguration. Successful implementation of the proposed method in real-world distribution systems requires addressing practical challenges such as data availability, communication infrastructure, and regulatory constraints.

Funding: This research was funded by the University of Washington Bothell SRCP Seed Grant#06-0398.

Informed Consent Statement: Not applicable.

Data Availability Statement: The datasets presented in this article are not readily available because the data are part of an ongoing study.

Conflicts of Interest: The author declares no conflicts of interest.

Nomenclature

$\varnothing_n$	AR coefficient of the ARMA model
θ_m	MA coefficient of the ARMA model
N	Order of the AR model
M	Order of the MA model
x_t	Wind speed/clearness index time series
μ_t	Mean of the wind speed/clearness index historical data
σ_t	Standard deviation of the wind speed/clearness index historical data
α_t	A zero mean, zero autocorrelation white noise with a variance of σ^2
W	Simulated wind speed
K	Simulated clearness index of solar radiation
P_{W-DG}	Output power of the wind DG
$P_{W-DG_{rated}}$	Rated power of the wind DG
v_{cut-in}	Cut-in speed of the wind turbine
$v_{cut-out}$	Cut-out speed of the wind turbine
v_{rated}	Rated speed of the wind turbine
P_{PV-DG}	Output power of the PV DG
A_{PV}	Area of the PV array
η_{PV}	Efficiency of the PV array
P_c	Charging power of the EV battery
P_d	Discharging power of the EV battery
P_c^{max}	Charging power rating of the EV battery
P_d^{max}	Discharging power rating of the EV battery
L	Number of time steps over the simulation period
MCP	Market clearing price
R_{EV}	Revenue for EV
R_{DG}	Revenue for renewable DG

PTC_{DG}	Production tax credit for renewable DG
PEN_{DG}	Penalties for renewable DG over-/-under production
$P_{Sch.-DG}$	Scheduled DG power
$P_{Act.-DG}$	Actual DG power
P_{Loss}	Total active power loss of the distribution grid
Q_{Loss}	Total reactive power loss of the distribution grid
N_{br}	Number of branches within the distribution grid
N_{ts}	Number of tie switches within the distribution grid
R_l	Resistance of the lth branch
I_l	Current of the lth branch
x_l	Status of the lth branch/tie switch (0 for open and 1 for close)
v_i^{min}	Minimum threshold of the voltage at bus i
v_i^{max}	Maximum threshold of the voltage at bus i
I_l^{max}	Maximum current capacity of the lth branch
N_b	Number of buses
P_i^{Gen}	Active power generation at bus i
P_i^{Load}	Active power consumption at bus i
Q_i^{Gen}	Reactive power generation at bus i
Q_i^{Load}	Reactive power consumption at bus i

References

1. Jian, L.; Zechun, H.; Banister, D.; Yongqiang, Z.; Zhongying, W. The future of energy storage shaped by electric vehicles: A perspective from China. *Energy* **2018**, *154*, 249–257. [CrossRef]
2. Liu, J.; Zhong, C. An economic evaluation of the coordination between electric vehicle storage and distributed renewable energy. *Energy* **2019**, *186*, 115821. [CrossRef]
3. Aliasghari, P.; Mohammadi-Ivatloo, B.; Alipour, M.; Abapour, M.; Zare, K. Optimal scheduling of plug-in electric vehicles and renewable micro-grid in energy and reserve markets considering demand response program. *J. Clean. Prod.* **2018**, *186*, 293–303. [CrossRef]
4. Alahyari, A.; Ehsan, M.; Mousavizadeh, M. A hybrid storage-wind virtual power plant (VPP) participation in the electricity markets: A self-scheduling optimization considering price, renewable generation, and electric vehicles uncertainties. *J. Energy Storage* **2019**, *25*, 100812. [CrossRef]
5. Gupta, K.; Narayanankutty, R.A.; Sundaramoorthy, K.; Sankar, A. Optimal location identification for aggregated charging of electric vehicles in solar photovoltaic powered microgrids with reduced distribution losses. *Energy Sources Part A Recover. Util. Environ. Eff.* **2020**, 1–16. [CrossRef]
6. Bruinsma, G.; Carati, E.G.; Piveta, M.; Salvatti, G.A.; Rech, C. Electric Vehicle Charging Strategy in Smart Grids with Distributed Generation. In Proceedings of the 2022 14th Seminar on Power Electronics and Control (SEPOC), Santa Maria, Brazil, 12–15 November 2022; pp. 1–6.
7. Sahoo, J.P.; Sivasubramani, S. A Charging Coordination Strategy for Seamless Integration of Plug-In Electric Vehicles into a Distribution Network. In Proceedings of the 2023 IEEE IAS Global Conference on Renewable Energy and Hydrogen Technologies (GlobConHT), Male, Maldives, 11–12 March 2023; pp. 1–6.
8. Zeynali, S.; Rostami, N.; Feyzi, M. Multi-objective optimal short-term planning of renewable distributed generations and capacitor banks in power system considering different uncertainties including plug-in electric vehicles. *Int. J. Electr. Power Energy Syst.* **2020**, *119*, 105885. [CrossRef]
9. Ghofrani, M.; Majidi, M. A comprehensive optimization framework for EV-Renewable DG coordination. *Electr. Power Syst. Res.* **2021**, *194*, 107086. [CrossRef]
10. Huang, Z.; Fang, B.; Deng, J. Muti-objective optimization strategy for distribution network considering V2G-enabled electric vehicles in building integrated energy system. *Prot. Control. Mod. Power Syst.* **2020**, *5*, 7. [CrossRef]
11. Salkuti, S.R. Optimal network reconfiguration with distributed generation and electric vehicle charging stations. *Int. J. Math. Eng. Manag. Sci.* **2021**, *6*, 1174–1185. [CrossRef]
12. Amin, A.; Tareen, W.U.K.; Usman, M.; Memon, K.A.; Horan, B.; Mahmood, A.; Mekhilef, S. An integrated approach to optimal charging scheduling of electric vehicles integrated with improved medium-voltage network reconfiguration for power loss minimization. *Sustainability* **2020**, *12*, 9211. [CrossRef]
13. Andervazh, M.-R.; Javadi, S.; Aliabadi, M.H. Active distribution network operation management with large penetration of hybrid electric vehicles and sustainable distributed energy generation. *Sustain. Cities Soc.* **2020**, *62*, 102313. [CrossRef]
14. Cheng, S.; Li, Z. Multi-objective network reconfiguration considering V2G of electric vehicles in distribution system with renewable energy. *Energy Procedia* **2019**, *158*, 278–283. [CrossRef]

15. Iea50- Electric Vehicle Charging and Grid Integration Tool. Available online: https://www.iea.org/data-and-statistics/data-tools/electric-vehicle-charging-and-grid-integration-tool (accessed on 29 March 2024).
16. MISO's Renewable Integration Impact Assessment (RIIA). Available online: https://cdn.misoenergy.org/RIIA%20Summary%20Report520051.pdf (accessed on 29 March 2024).
17. Singh, B.; Pozo, D. A guide to solar power forecasting using ARMA models. In Proceedings of the 2019 IEEE PES Innovative Smart Grid Technologies Europe (ISGT-Europe), Bucharest, Romania, 29 September–2 October 2019; pp. 1–4.
18. Sansa, I.; Boussaada, Z.; Bellaaj, N.M. Solar radiation prediction using a novel hybrid model of ARMA and NARX. *Energies* **2021**, *14*, 6920. [CrossRef]
19. Ghofrani, M.; Arabali, A.; Etezadi-Amoli, M.; Fadali, M.S. Smart scheduling and cost-benefit analysis of grid-enabled electric vehicles for wind power integration. *IEEE Trans. Smart Grid* **2014**, *5*, 2306–2313. [CrossRef]
20. Rogers, J.; Porter, K. *Wind Power and Electricity Markets, a Living Summary of Markets and Market Rules for Wind Energy and Capacity in North America*; Utility Wind Integration Group: Reston, VA, USA, 2011.
21. Brekken, T.K.A.; Yokochi, A.; von Jouanne, A.; Yen, Z.Z.; Hapke, H.M.; Halamay, D.A. Optimal energy storage sizing and control for wind power applications. *IEEE Trans. Sustain. Energy* **2010**, *2*, 69–77. [CrossRef]
22. Section G3: Operating requirements for transmission generating entities. PG&E Transmission Interconnection Handbook. 2023. Available online: https://www.pge.com/assets/pge/docs/about/doing-business-with-pge/g3.pdf (accessed on 29 March 2024).
23. Yimam, F.A. Genetic Algorithm-Based Distribution Network Reconfiguration for Power Loss Reduction. Master's Thesis, Addis Ababa Science and Technology University, Addis Ababa, Ethiopia, 2020.
24. Pereira, R.A.F.; da Silva, L.G.W.; Kezunovic, M.; Mantovani, J.R.S. Improved fault location on distribution feeders based on matching during-fault voltage sags. *IEEE Trans. Power Deliv.* **2009**, *24*, 852–862. [CrossRef]